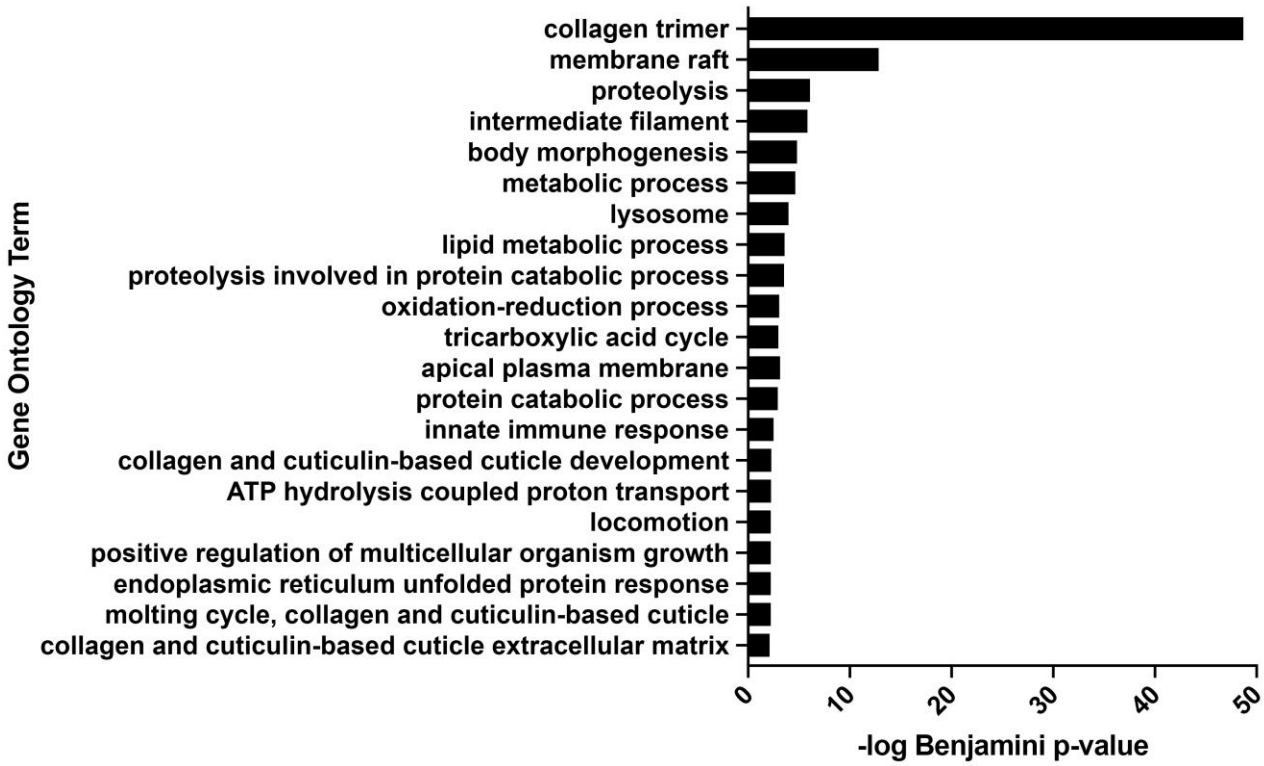

Supplementary Figure 1

GO analysis of Parkinson's disease predictions.

GO enrichment analysis as performed on PD predictions with a score > 2.0 (n=609 genes). Significant GO terms are shown. Bars represent individual Benjamini p-values derived from GO enrichment analysis.

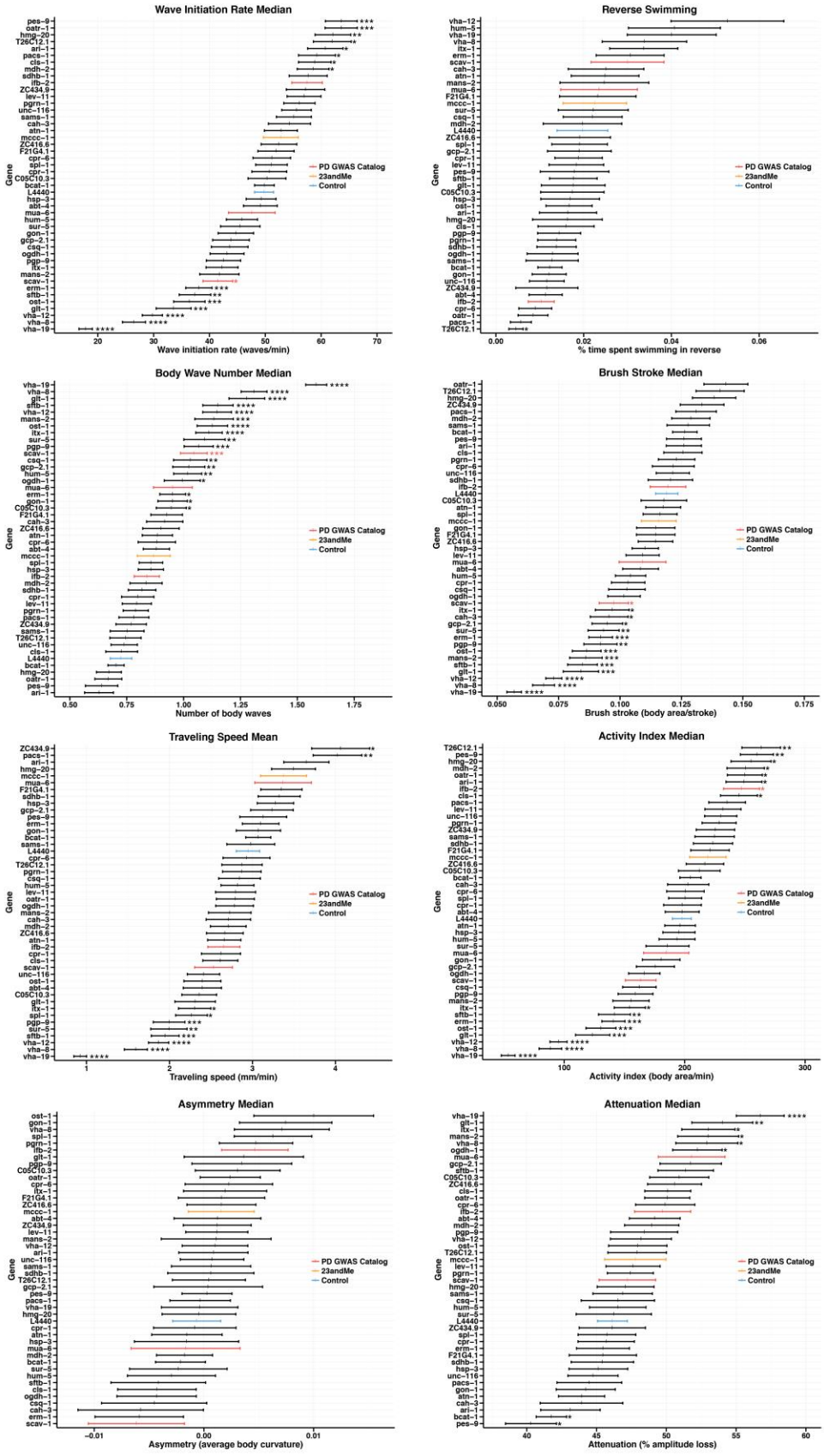

Nature Biotechnology: doi:10.1038/nbt.4246

Supplementary Figure 2

Thrashing phenotypes of candidate Parkinson's disease genes.

Neuron-sensitive animals (*unc-119p::sid-1*) were exposed to adult-only RNAi targeting 45 top candidate PD genes, and tested for thrashing defects on days 2, 5, and 8 of adulthood. Movement was analyzed using CeleST. CeleST quantification of thrashing on day 8 is shown. Control L4440 RNAi (blue), direct GWAS worm orthologs (red), and candidates independently identified using the 23andMe GWAS study (yellow) are shown. Mean ± SEM, unpaired two-sided t-test, Benjamini-Hochberg multiple hypothesis test correction, n ≥ 50 per gene (exact sample sizes per gene in Supplementary Data 13). *p<0.05, **p<0.01, ***p<0.001, ****p<0.0001.

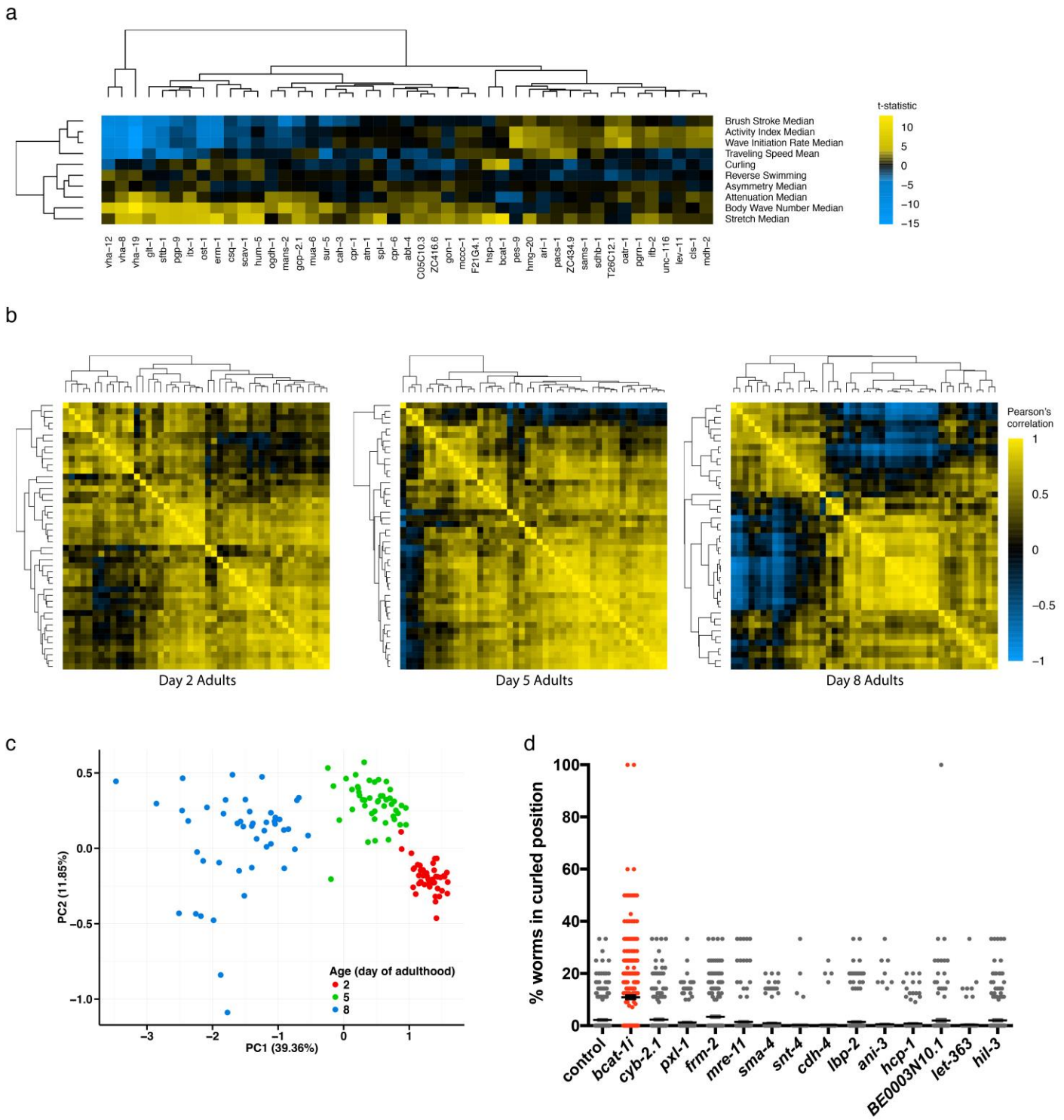

Supplementary Figure 3

Screen of Parkinson's disease–candidate genes for age-specific motor defects.

Animals were exposed to adult-only RNAi targeting 45 top candidate PD genes, and tested for thrashing defects on days 2, 5, and 8 of adulthood. Movement was analyzed using CeleST. **(a)** Heatmap of (hierarchically clustered) t-statistics comparing 10 CeleST movement measurements for each of the top 45 top PD gene candidates against the control L4440 RNAi on day 8 of adulthood, n ≥ 50

per gene (exact sample sizes per gene in Supplementary Data 13). **(b)** Pearson's correlation of t-statistics for each of the 10 CeleST movement measurements between all pairs of genes tested on days 2, 5, and 8 of adulthood. **(c)** Principal components were calculated using all 13,048 worms (across 45 genes and 3 days). PCA plot of RNAi-treated worms and control (aggregated by gene and day, see sample sizes in Supplementary Data 13). Colors indicate age of worm. PC1 (x-axis) and PC2 (y-axis) respectively account for 39.36% and 11.85% of the total variation. **(d)** Neuronal RNAi-sensitive animals were exposed to adult-only RNAi individually targeting 13 top cancer and metabolic disease predictions, *bcat-1* (red) as a positive control, or the L4440 negative control. Curling was examined on day 8 using an automated analysis program (Sohrabi, et al. in preparation). Mean ± SEM. Control n=351, *bcat-1* n=420, *cyb-2.1* n=287, *pxl-1* n=289, *frm-2* n=279, *mre-11* n=272, *sma-4* n=286, *snt-4* n=305, *cdh-4* n=285, *lbp-2* n=320, *ani-3* n=300, *hcp-1* n=264, *BE0003N10.1* n=229, *let-363* n=284, *hil-3* n=270. n represents the number of animals per condition. One-way ANOVA with Tukey's multiple comparisons test. Control vs *bcat-1i* p= 4.33e-8. ****p<0.0001.

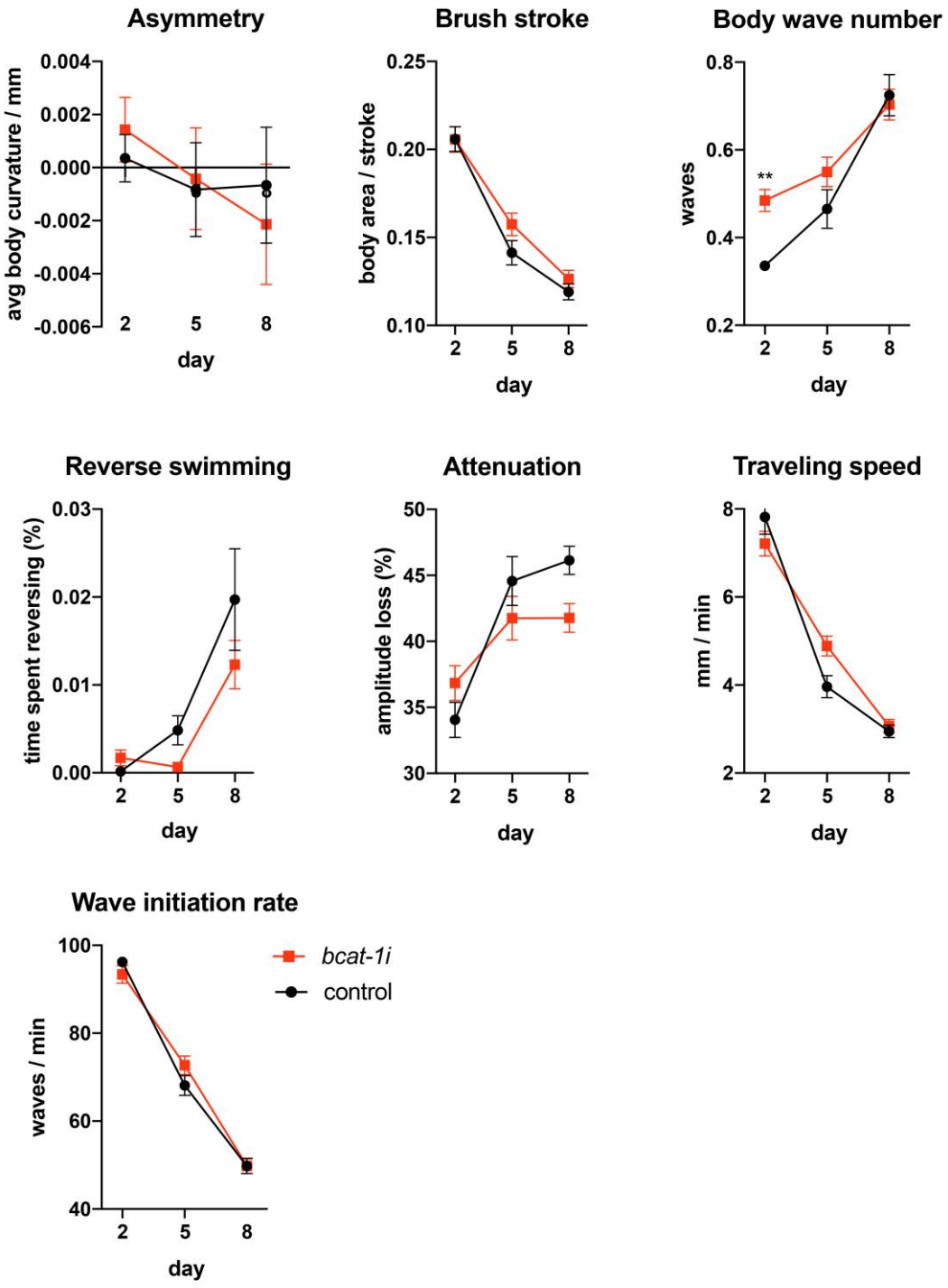

Supplementary Figure 4

Age-related thrashing of *bcat-1* RNAi-treated animals.

CeleST was used to analyze control and *bcat-1* RNAi-treated worms on day 2, 5, and 8 of adulthood. Mean ± SEM, two-way ANOVA with Sidak's multiple comparisons test, Control: day 2 n=492, day 5 n=345, day 8 n=573. *bcat-1* RNAi: day 2 n=675, day 5 n=714, day 8 n=582. Body wave number day 2 control vs *bcat-1i*: t=3.075, df=3375, 95% CI: (-0.2648, -0.03323), p=0.0064.

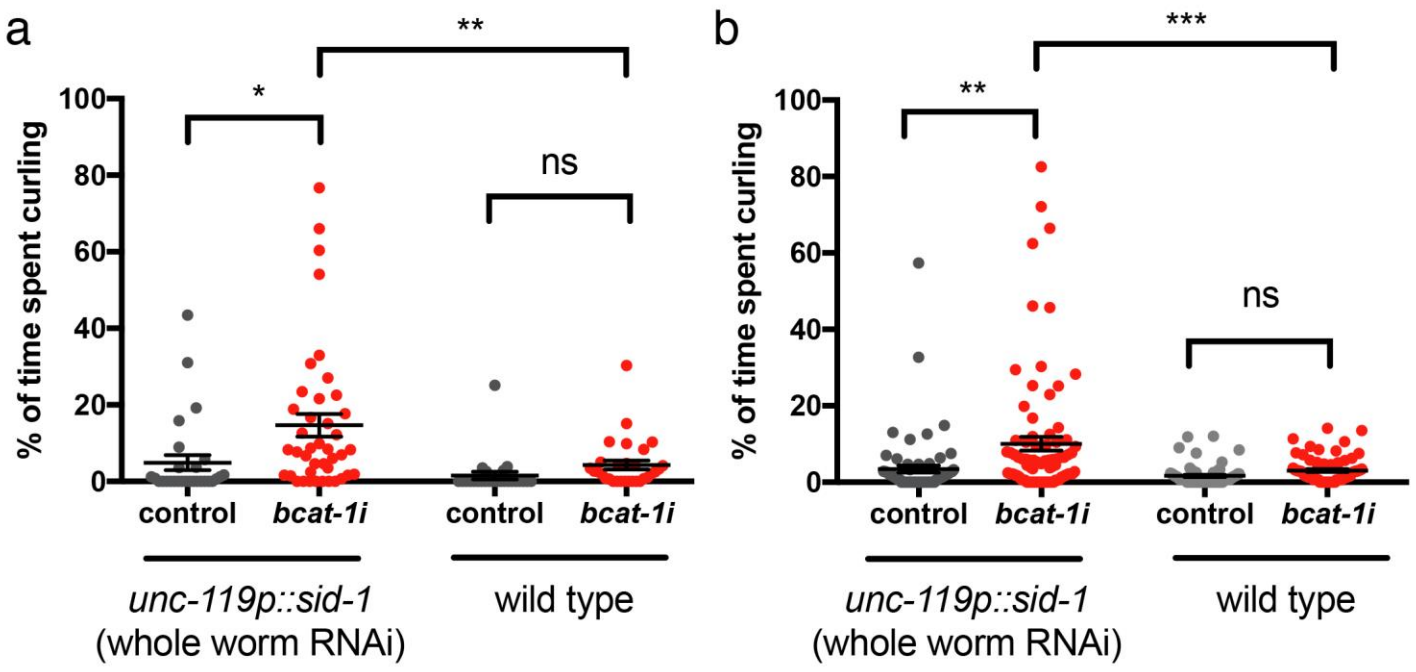

Supplementary Figure 5

Neuron RNAi sensitivity is required for *bcat-1*-mediated curling.

Neuron RNAi insensitive, wild-type (N2) worms treated with control (L4440) or *bcat-1* RNAi do not exhibit curling on Day 8 of adulthood compared to neuron-RNAi sensitive animals (*unc-119p::sid-1)*. Mean ± SEM, *p<0.05, **p<0.01, ***p<0.001, ****p<0.0001, two-way repeated measures ANOVA, Tukey's post hoc tests. Worm thrashing videos were hand counted. **(a)** Control;*unc-119p::sid-1* n=28 animals, *bcat-1i:unc-119p::sid-1* n=41 animals, control;wild type n=24 animals, *bcat-1i*;wild type n=30 animals. Multiple comparisons: Control:*unc-119p::sid-1* vs. *bcat-1i:unc-119p::sid-1* t=3.156, df=119, 95% CI: (-18.7, -1.491), p=0.0121. Control:wild type vs. *bcat-1i*:wild type t=0.7787, df=119, 95% CI: (-11.98, 6.577), p=0.9684. *bcat-1i*:*unc-119p::sid-1* vs. *bcat-1i*:wild type t=3.422, df=119, 95% CI: (2.272, 18.55), p=0.0051. **(b)** Control;*unc-119p::sid-1* n=75 animals, *bcat-1i:unc-119p::sid-1* n=86 animals, control;wild type n=73 animals, *bcat-1i*;wild type n=76 animals. Multiple comparisons: Control:*unc-119p::sid-1* vs. *bcat-1i:unc-119p::sid-1* t=4.305, df=306, 95% CI: (-10.68, -2.546), p=0.000135. Control:wild type vs. *bcat-1i*:wild type t=0.8621, df=306, 95% CI: (-5.595, 2.847), p=0.948. *bcat-1i*:*unc-119p::sid-1* vs. *bcat-1i:*wild type t=4.576, df=306, 95% CI: (2.952, 11.06), p=0.00041.

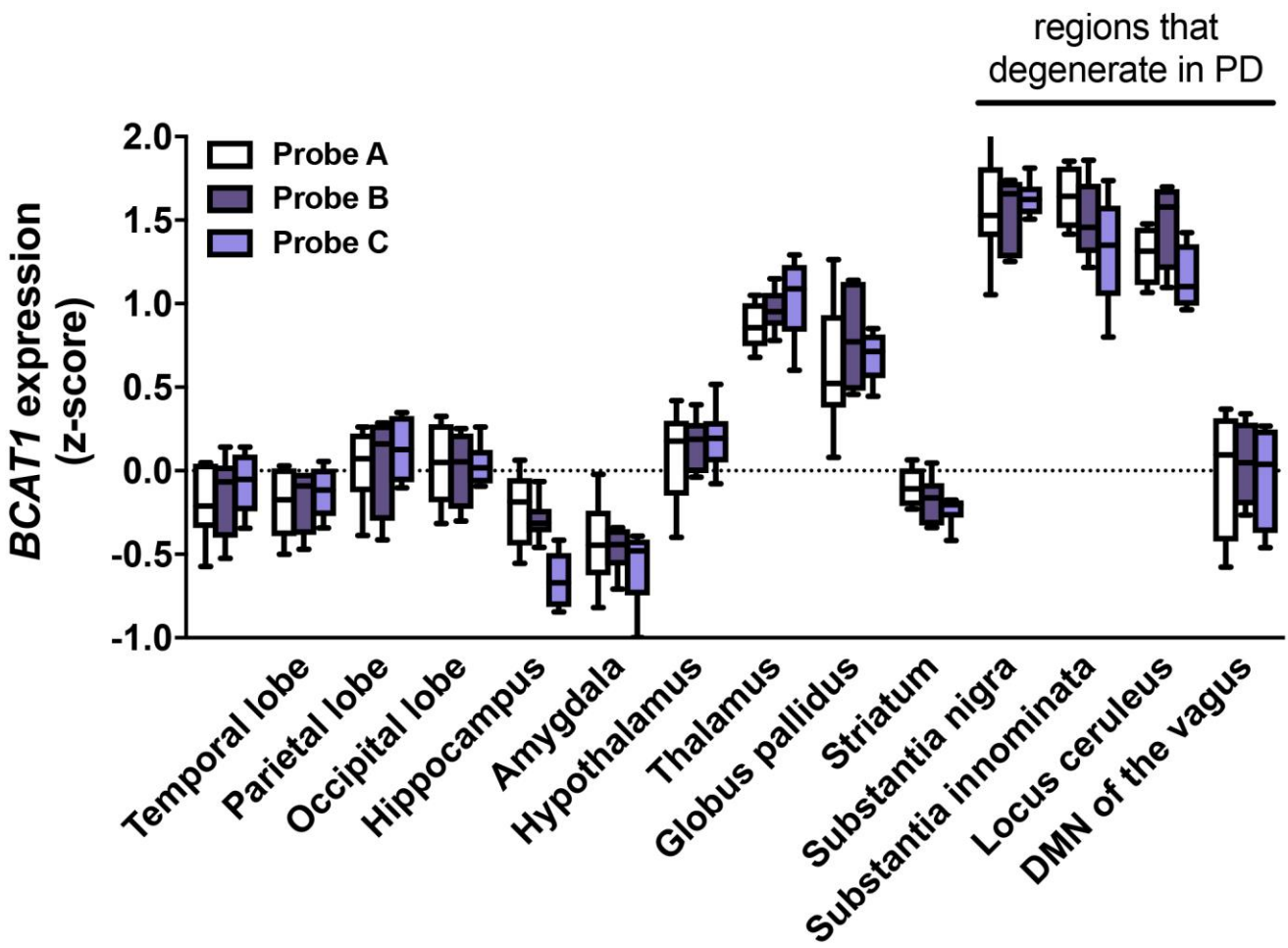

Supplementary Figure 6

BCAT1 expression in selected brain regions in healthy human subjects from the Allen Brain Atlas.

Average *BCAT1* expression in selected brain regions of healthy human individuals, obtained from the Allen Brain Atlas. Expression data for each of three *BCAT1* probes is shown for several major brain regions, in addition to four regions that degenerate in PD. Probe A, A_23_P87528; Probe B, A_24_P52921; Probe C, A_24_P935986. Mean ± SEM. n=6 human donors for each sample from the Allen Brain Atlas database for gene expression. Box plots show minimum, first quartile, median, third quartile, and maximum values.

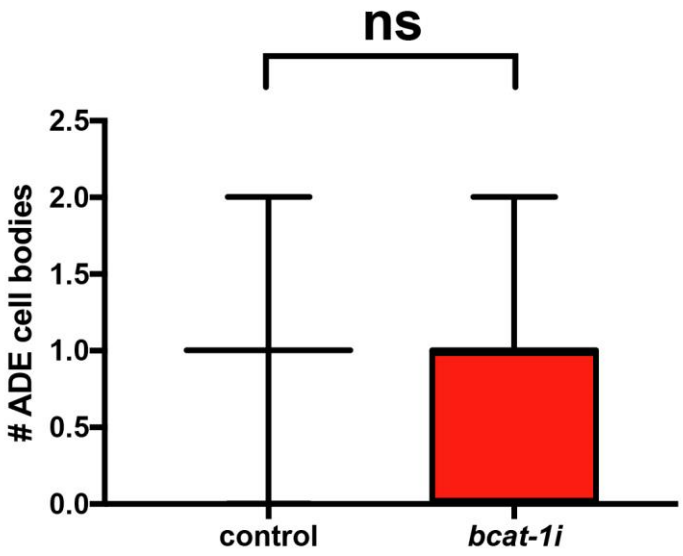

Supplementary Figure 7

bcat-1 knockdown does not alter ADE cell-body numbers in the presence of α-synuclein.

ADE cell bodies were counted on Day 8 in neuron-RNAi sensitive worms expressing α-synuclein and GFP in dopaminergic neurons. Mean ± SEM, unpaired two-sided Student's t-test. L4440 n=45 animals, *bcat-1i* n=61 animals. t=0.4156, df=104, 95% CI: (-0.3112, 0.2033), p=0.6785. The experiment was repeated three times independently with similar results. Box plots show minimum, first quartile, median, third quartile, and maximum values.

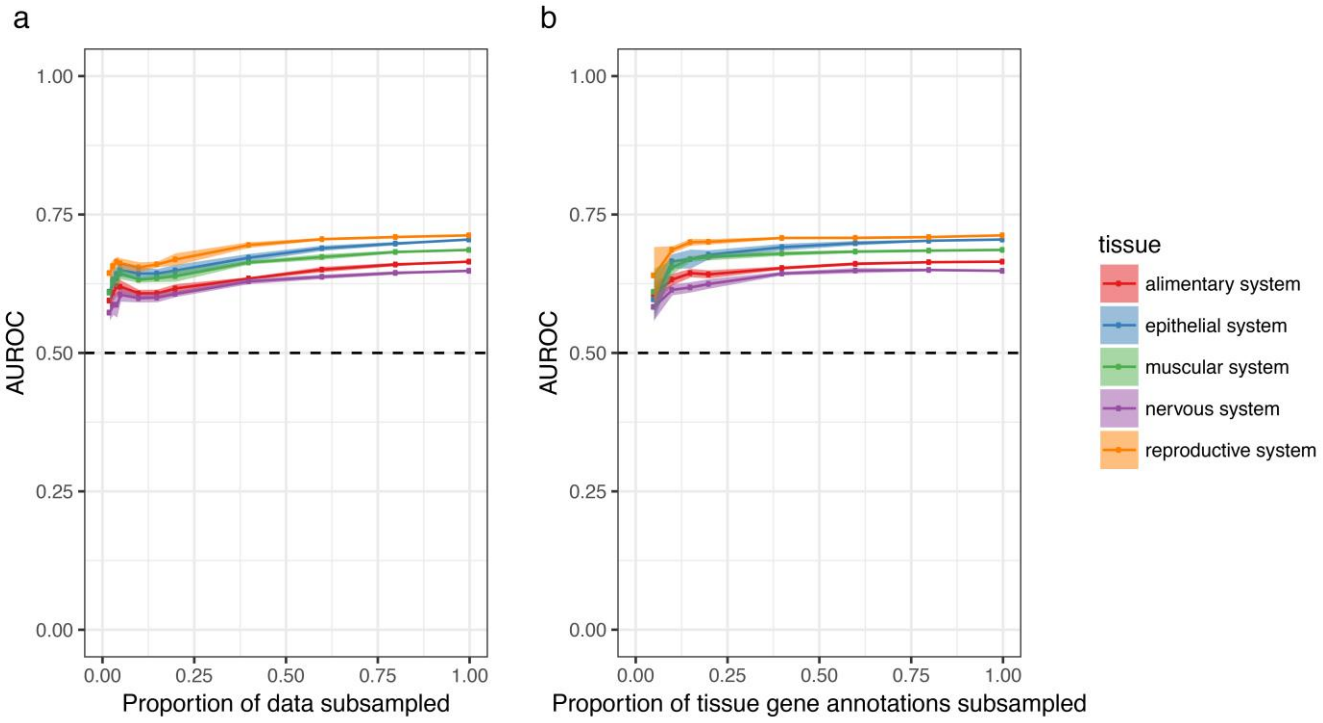

Supplementary Figure 8

The Functional Representation module is robust to data compendium size, amount of prior knowledge, and initialization state.

Semi-supervised network construction approach was applied to **(a)** ten progressively smaller compendia sub-sampled from the full worm compendium (without replacement) and **(b)** seven progressively smaller sets of tissue gene annotations subsampled from all previously known tissue genes (without replacement). Each measurement is an average of 10 independent simulations and standard error (shaded regions) is shown.